New Method for Determining Dielectric Properties of Skin and Phantoms at Millimeter Waves Based on Heating Kinetics

Nacer Chahat, *Student Member, IEEE*, Maxim Zhadobov, *Member, IEEE*, Ronan Sauleau, *Senior Member, IEEE*, and Stanislav I. Alekseev, *Member, IEEE*

***Abstract*—Recent progress in millimeter-wave (MMW) wireless body-centric applications triggered an increasing interest to characterize the interactions between the millimeter waves and the human body. The determination of the dielectric properties of skin and phantoms (artificial models with tissue-equivalent dielectric properties) at MMW is crucial for the accurate evaluation of the power absorption and distribution in the skin. In this study, we show that the heating kinetics resulting from the MMW exposure can be used for the accurate determination of the penetration depth (δ) and power density (I) in different samples (1% and 4% agar phantoms, 20% and 25% polyethylene powder (PEP) phantoms, and human skin). The samples have been exposed at 60.4 GHz using an open-ended waveguide. The temperature distribution and dynamics are recorded using an infrared camera. The values of δ and I are defined by fitting the analytical solution of the bio-heat transfer equation to the experimental heating kinetics. The values of δ are further used to retrieve the permittivity spectra of materials described by Debye equation. Simultaneously, δ is calculated using the permittivity directly measured using a slim coaxial probe. Both results are in good agreement. Finally, our results demonstrate that the permittivity of a 20% PEP phantom is close to that of skin. Hence, this phantom can be used to model the MMW interactions with skin and to characterize on-body wearable MMW antennas.**

***Index Terms*—Body-centric applications, experimental phantoms, human skin permittivity, infrared thermometry, permittivity measurement.**

I. Introduction

RECENTLY, the body area networks (BANs) operating in the unlicensed 57–64-GHz band have been identified as a highly promising solution since they provide several advantages compared with microwave BANs. First, very high data rates can be reached (typically up to 5 Gb/s) because of the large available spectrum (7 GHz worldwide) [1]. Second, high free-space losses due to the atmospheric oxygen-induced absorption around 60 GHz result in a high level of security and low interference with adjacent networks [2]. Finally, the size of on-body devices is greatly reduced compared with similar systems operating at microwaves.

The extension of BAN to the millimeter-wave (MMW) range requires careful characterization of the antenna/human body interaction in order to evaluate, and possibly minimize, the variations of antenna characteristics and exposure levels induced to the body. To this end, knowledge of the dielectric properties of the human tissues is crucial for the numerical modeling and development of experimental phantoms [3]. Any variations of the dielectric properties could directly impact the theoretical and experimental results.

Several techniques have been introduced so far to determine the complex permittivity of skin at MMW. Gabriel *et al.* [4] reported extrapolated permittivity values up to 110 GHz based on human skin measurements performed below 20 GHz using an open-ended coaxial probe ($\varepsilon^*_{60\mathrm{GHz}} = 7.98 - j10.90$). Gandhi *et al.* presented results at 60 GHz [5] obtained with a Debye model relying on measurements performed on rabbit skin at 23 GHz ($\varepsilon^*_{60\mathrm{GHz}} = 8.89 - j13.15$). Alabaster *et al.* used a free-space technique on excised samples of human skin at 60 GHz ($\varepsilon^*_{60\mathrm{GHz}} = 9.9 - j9.0$) [6]. Hwang *et al.* [7] measured the human skin permittivity *in vivo* up to 110 GHz using a coaxial probe ($\varepsilon^*_{60\mathrm{GHz}} = 8.05 - j4.13$). Alekseev *et al.* [8] carried out reflection measurements using an open-ended waveguide and proposed homogeneous and multilayer human skin models fitting the experimental data ($\varepsilon^*_{60\mathrm{GHz}} = 8.12 - j11.14$).

The reported skin permittivity data strongly depend on a number of parameters, including the measurement technique, the sample under test, and the location on the body [9]. Furthermore, direct electromagnetic measurements at MMW often require quite sophisticated and costly equipment, such as a MMW vector network analyzer. Development of alternative permittivity measurement techniques is important, particularly at MMW frequencies, to reduce the measurement cost and validate the accuracy of available data.

Besides, skin-equivalent experimental phantoms have been developed very recently for on-body characterization of wearable MMW antennas [3]. Changes of the phantom dielectric properties with time, related for instance to evaporation, also requires accurate, and noninvasive measurement of its dielectric properties.

This paper proposes a new method for determining the dielectric properties of skin and phantoms at MMW based on the measurements of the heating kinetics. Compared with most of the existing techniques, this method allows performing nondestructive measurements *in situ*.

Manuscript received July 01, 2011, revised October 24, 2011; accepted November 08, 2011. Date of publication January 04, 2012; date of current version March 02, 2012. This work was supported in part by "Agence Nationale de la Recherche" (ANR), France under Grants ANR-09-RPDOC-003-01 (Bio-CEM project) and by "Centre National de la Recherche Scientifiques (CNRS)," France.

N. Chahat, M. Zhadobov, and R. Sauleau are with the Institute of Electronics and Telecommunications of Rennes (IETR), UMR CNRS 6164, University of Rennes 1, 35042 Rennes, France (e-mail: nacer.chahat@univ-rennes1.fr).

S. I. Alekseev is with the Institute of Cell Biophysics, Russian Academy of Sciences, 142292 Pushchino, Russia.

Digital Object Identifier 10.1109/TMTT.2011.2176746

The paper is organized as follows. The considered samples, measurement setup, and methodology are described in Section II. The results are given in Section III for different materials and are compared with data obtained from reflection measurements. Finally, the proposed method is discussed in detail in Section IV.

II. Materials and Methods

A. Samples Description

The penetration depth and the complex permittivity of the following samples have been determined: 1) two agar phantoms; 2) two polyethylene powder (PEP) phantoms; and 3) human skin. They are described in detail hereafter.

First, we have considered two phantoms made of distilled water and 1% or 4% agar. Due to the high water concentration, the permittivity of these phantoms is close to the permittivity of free water ($\varepsilon^*_{\text{water}} = 11.9 - j19.5$ at 60 GHz, 20 °C) [10].

Second, 20% and 25% PEP phantoms have been investigated. They are prepared by adding PEP, agar, and TX-151 into distilled water. TX-151 is a white powder that solidifies when mixed with water to obtain a material with the consistency of rubber. Such phantoms have been widely used to model human tissues at microwave frequencies [11], [12]. Recently, a skin-equivalent PEP phantom has been developed for modeling human skin in the 55–65-GHz range [3].

All phantoms have a cylindrical shape with a thickness of 2 cm and a diameter of 14 cm, and they are at ambient temperature.

Finally, measurements have been performed on the forearm skin. Three volunteers from the laboratory staff participated in these experiments. All volunteers have a solid background in electromagnetics and were informed about the purpose of the measurements.

B. Measurement Setup

The experimental setup is represented in Fig. 1. Phantoms and skin are exposed at 60.4 GHz using a WR-15 rectangular open-ended waveguide (9 dBi gain) located at 17 mm above the object. A CW signal is generated by a narrowband Gunn oscillator. After amplification, the signal is transmitted towards the waveguide aperture. The input power P_{in} of the radiating waveguide (Fig. 1) equals 425 mW. Similar power levels are commonly used in bioelectromagnetic studies [9]. The input power is controlled and adjusted before each experiment using an Agilent E4418B power meter (Agilent Technologies, Santa Clara, CA).

A FLIR SC5000 high-resolution infrared (IR) camera (FLIR Systems, Wilsonville, OR) operating in the 2.5–5.1-μm spectral range is used for recording the heating pattern and dynamics on the surface of exposed samples at the ambient temperature ($20°\text{C}$). The thermal sensitivity of the camera provided by the manufacturer is 0.025 °C. The IR camera allows obtaining images with a spatial resolution up to 640×512 pixels. Under the experimental conditions considered in this study, the resolution on the sample surface is roughly 0.2 mm^2. The sequence of thermal images is recorded at a sampling rate of 25 frames per second. We would recommend the following minimal requirements on the camera features for the proposed technique: 1) resolution on the sample: 1 mm^2; 2) frame rate: 10 Hz; and 3) thermal resolution: 0.1 °C.

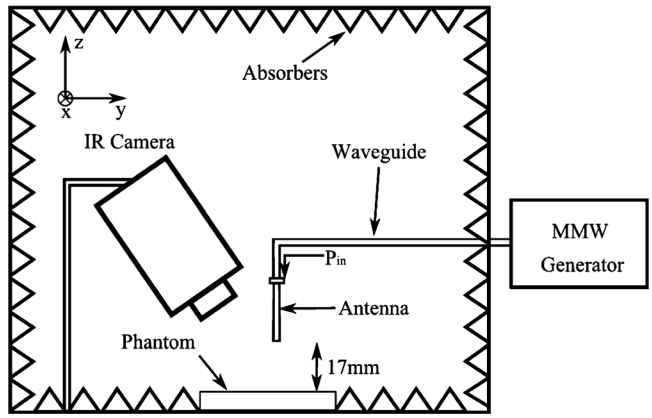

Fig. 1. Schematic representation of the measurement set-up (proportions are not to scale). The main parts of the millimeter-wave generator (QuinStar Technology Inc.) are the following: 1) 60.42-GHz tunable Gunn oscillator; 2) V-band tunable attenuator; 3) V-band power amplifiers (25 dB gain); 4) isolator (20 dB isolation).

C. Methodology

The proposed methodology is divided in two parts. First, we describe the approach implemented for the determination of the penetration depth of the considered samples. Second, the procedure implemented to retrieve the permittivity spectrum is provided.

1) Determination of the Penetration Depth: It was shown previously that the initial temperature rise rate of the heating kinetics does not depend on the exposing beam size (e.g., open-ended waveguide or horn antenna) if the peak incident power density is kept at the same level [14]. Therefore, the heating of the skin or phantom can be modeled by the following 1-D bio-heat transfer equation (BHTE) [15]:

$$\rho C \cdot \frac{\partial T_t}{\partial t} = k \cdot \frac{\partial^2 T_t}{\partial z^2} - V_s \cdot (T_t - T_b) + Q(z,t) \qquad (1)$$

where T_t is the tissue (or phantom) temperature, T_b is the arterial blood temperature, ρ is the mass density, C is the specific heat of the exposed material, k is the heat conduction coefficient, $V_s = f_b \cdot \rho_b \cdot C_b$, where f_b is the specific blood flow rate (equal to 0 for the considered phantoms), ρ_b and C_b are the density and specific heat of blood, respectively, and $Q(z,t)$ is the heat deposition from the MMW exposure, where z is the direction of penetration (normal to the sample interface). Further, we will consider the relative temperature rise $T = T_t - T_b$.

The heat deposition in skin or phantom can be defined as follows [15]:

$$Q(z,t) = \frac{2 \cdot (1-R)}{\delta} \cdot I_o \cdot e^{-2z/\delta} \cdot u(t) \qquad (2)$$

where R is the power reflection coefficient, I_o is the incident power density, and $u(t)$ is the unit step function.

Equation (1) is solved analytically under the following boundary conditions:

$$T(\infty,t)=0, \qquad t\geq 0$$
$$\frac{\partial T(0,t)}{\partial z}=\alpha(T+T_b-T_e), \qquad t\geq 0 \tag{3}$$

where $\alpha = h/k$, h is the heat transfer coefficient describing the heat loss from the sample to the external environment due to radiation, convection, and evaporation [16] and T_e is the ambient temperature. The initial conditions are determined from the steady-state solution of (1) at $Q(z,t)=0 (t\leq 0)$ as

$$T(z,0)=\alpha\frac{(T_e-T_b)}{\alpha+\sqrt{\lambda}}e^{-z\sqrt{\lambda}} \tag{4}$$

where $\lambda = V_s/k$.

The transient solution for the temperature rise on the surface of a homogeneous and isotropic semi-infinite medium (i.e., at $z=0$) is given by

$$\begin{aligned}T(t)=\frac{q}{\lambda-1/L^2}\Bigg\{&1+\frac{1/L+\alpha}{2\left(\sqrt{\lambda}-\alpha\right)}\cdot erfc\left(\sqrt{\frac{\lambda t}{\mu}}\right)-\frac{(1/L+\alpha)}{2(\sqrt{\lambda}+\alpha)}\\&\cdot erfc\left(-\sqrt{\frac{\lambda t}{\mu}}\right)-\frac{1}{2}\exp\left(\frac{t}{\mu}\left(\frac{1}{L^2}-\lambda\right)\right)\\&\cdot erfc\left(\frac{1}{L}\sqrt{t/\mu}\right)-\frac{(1/L+\alpha)}{2\,(1/L-\alpha)}\\&\cdot\exp\left(\frac{t}{\mu}\left(1/L^2-\lambda\right)\right)\cdot erfc\left(\frac{1}{L}\sqrt{t/\mu}\right)\\&+\frac{\alpha\left(\lambda-1/L^2\right)}{(\lambda-\alpha^2)\left(\frac{1}{L}-\alpha\right)}\cdot\exp\left(\left(\alpha^2-\lambda\right)\frac{t}{\mu}\right)\\&\cdot erfc\left(\alpha\sqrt{t/\mu}\right)\Bigg\}+\frac{\alpha\,(T_e-T_b)}{\alpha+\sqrt{\lambda}}\end{aligned} \tag{5}$$

where $\mu=\rho C/k$, $q=2(1-R)I_o/(\delta\cdot k)$, and $L=\delta/2$. This solution is in agreement with that given in [15].

Some parameters appearing in the expression of $T(t)$, such as ρ, C, k, and f_b, are well established and given in the literature. The heat transfer coefficient h can be easily calculated [16]. If we define the absorbed power density as $I=(1-R)I_0$, then the number of unknown parameters in (5) is reduced to two, namely, δ and I.

To determine δ in the considered samples, we first measure the temperature increase as a function of time with the IR camera during 10 s of exposure. Then, using the least-squares technique, we fit these experimental data to the theoretical model $T(t)$ by varying δ and I. In practice, only one temperature recording is sufficient, as the measurement results are reproducible. The standard deviation (SD) between the experimental data and the theoretical model $T(t)$ as a function of δ and I, has only one minimum. This means that there is a unique set of values for δ and I corresponding to the experimental heating kinetics for a given sample.

As an example, Fig. 2 represents the SD for the 20% PEP phantom. The minimum SD is obtained for $\delta = 0.48mm$ and $I = 77.8\text{mW/cm}^2$. More detailed results for this phantom are given and discussed in Section III.

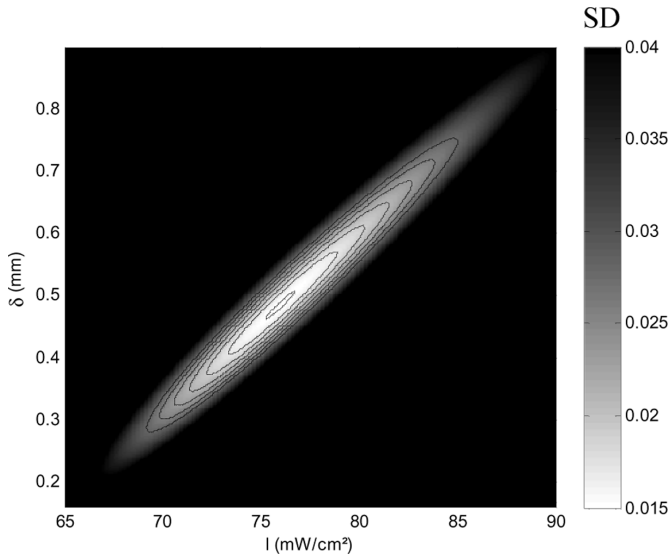

Fig. 2. Standard deviation between the experimental data and the theoretical model $T(t)$ as a function of δ and I. The temperature kinetics was obtained for 20% PEP exposed at 60.4 GHz.

This approach allows us to determine the penetration depth δ for each sample under test at 60.4 GHz.

2) Retrieval of the Complex Permittivity: The penetration depth determined above at 60.4 GHz is used for the calculation of the complex permittivity spectrum of each sample. It can be expressed as follows [17]:

$$\delta=\frac{c}{2\pi\cdot f\cdot \mathrm{Im}(\sqrt{\varepsilon*})} \tag{6}$$

where c is the velocity of light in free space and f is the frequency.

It is well known that the relaxation frequencies of all components in biological tissues (e.g., proteins, lipids, or bound water), except free water, lie below 5 GHz. Therefore, those of biological tissues at MMW are close to the relaxation frequencies of free water at the same temperature [4], [5], [8]. It is also known that the skin permittivity at MMW can be described by a Debye model [17]

$$\varepsilon^*=\varepsilon'-j\varepsilon''=\varepsilon_\infty+\frac{\Delta\varepsilon}{1+j\omega\tau}+\frac{\sigma}{j\omega\varepsilon_0} \tag{7}$$

where τ is the relaxation time equal to that of free water, $\omega = 2\pi f$, $j=(-1)^{1/2}$, $\Delta\varepsilon=\varepsilon_s-\varepsilon_\infty$ is the magnitude of the dispersion of the free water fraction of the sample, ε_s is the permittivity at $\omega\tau \ll 1$, ε_∞ is the optical permittivity, $\varepsilon_0 = 8.85\times10^{-12}\ \mathrm{F/m}$, and σ is the ionic conductivity. The optical permittivity ε_∞ equals $2.5+2.7w_t$, where w_t is the weight fraction of the total water content of the material to be characterized [18].

In [8], the authors determined $\Delta\varepsilon$ in (7) by fitting the theoretical power reflection coefficient to the experimental data. In the current study, we use a similar approach to determine $\Delta\varepsilon$ and therefore $\varepsilon*$. Varying $\Delta\varepsilon$ in the Debye equation (7), we can find the optimized value of $\Delta\varepsilon$ for which the penetration depth δ given by (6) is equal to that found from the temperature kinetics measurements (δ_1).

To illustrate this technique, we consider here the 20% PEP phantom. The penetration depth δ_1, calculated from the temperature kinetics, equals 0.48 mm. The parameters of the Debye model have been optimized to obtain the same penetration depth: $\Delta\varepsilon = 39.0$, $\tau = 9.27 \cdot 10^{-12}$ s, $\varepsilon_\infty = 4.5$ ($w_t = 0.8$ for this phantom), and $\sigma = 0$ (the phantom employed in this study does not contain salts and free ions). The resulting penetration depth δ equals exactly 0.48 mm. The permittivity results for the optimized Debye model are presented in detail in Section III (cf. Fig. 4).

To cross check the permittivity results and to validate the proposed methodology, an open-ended coaxial slim probe operating up to 67 GHz has been used for the permittivity measurements applying the methodology provided in [13].

III. Results

Fig. 3 represents the temperature distribution and dynamics for the 20% PEP phantom illuminated by the open-ended waveguide within the compact anechoic chamber presented in Fig. 1. The heated area of the phantom has a circular shape [Fig. 3(a)], and the temperature profile has a Gaussian-type distribution [Fig. 3(b)]. The diameter of the heated spot at -3 dB level of the peak temperature is equal to 12 mm. The solution of the 1-D BHTE fitted to the experimental temperature kinetics is plotted in Fig. 3(c). Similar heating patterns and good match of the theoretical kinetics to the experimental data have been also obtained for the other samples under test.

The penetration depths δ_1 at 60.4 GHz found from the fitting procedure (Section II-C) are given in Table I for all samples considered here. The thermo-physical parameters used in these calculations (Table I) were selected in accordance with the literature data [11], [18], [19]. In the same table, we also give the penetration depths δ_2 obtained from direct measurements of permittivity using an open-ended slim coaxial probe. Both sets of results demonstrate a very good agreement. As expected, in 1% agar phantom, the penetration depth is equal to that of water ($\delta_{\text{water}} = 0.318$ mm at 20 °C) [10]. The experimental results obtained with the other samples confirm that this method can be applied for the determination of δ for materials with a relatively wide range of the permittivity values.

In addition, the penetration depth in skin has been calculated analytically using the skin permittivity values provided by Gabriel *et al.* [4]. Using these data, the calculated penetration depth equals 0.48 mm; it is very close to our results for the penetration depth in skin (Table I).

The value of δ which is the closest to the penetration depth in skin [4] is obtained for the 20% PEP phantom. Fig. 4 represents the permittivity spectrum of this phantom when measured directly using the slim coaxial probe and the one retrieved from the heating kinetics. The results are in very good agreement ($\Delta\varepsilon' = 0.2[2.6\%]$ and $\Delta\varepsilon'' = 0.6[6.1\%]$ at 60 GHz).

Although the distance between the waveguide aperture and the sample surface was maintained constant, the maximal temperature elevation during 10 s of exposure was different for the selected samples. Though these elevations strongly depend on the material reflectivity and heat transfer coefficients, the variations in heating do not well correlate with changes in reflectivity and h. We presume that this is due to the difference in the material emissivity. However, these variations in heating do not change the values of δ obtained during the fitting procedure, and therefore they do not impact the retrieved permittivity spectra. At the same time, the contribution of the emissivity should be carefully taken into account for the accurate determination of I that is proportional to the temperature increment. As the temperature monitored by an IR camera directly depends on the emissivity, the use of incorrect values of emissivity may result in errors when determining I.

Taking into account that the emissivity of skin is close to 1 [19], we calculated the incident power density I_0 for the skin

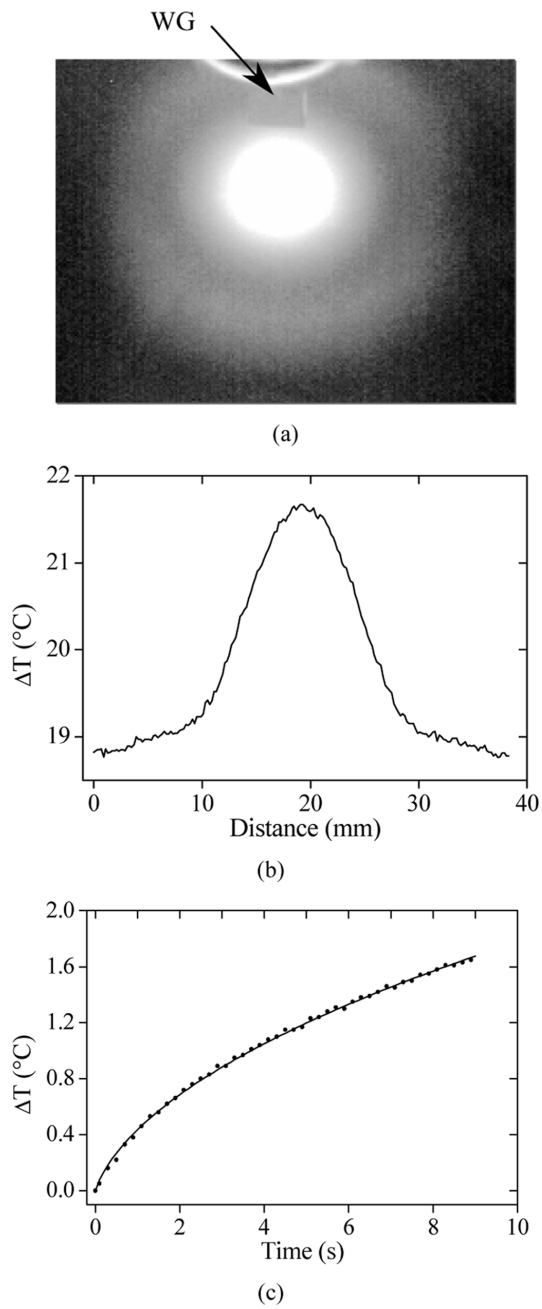

Fig. 3. Heating profiles and dynamics for the 20% PEP phantom. (a) IR image of the temperature distribution on the surface of phantom exposed at 60.4 GHz by an open-ended waveguide (WG). (b) Temperature profile in the cutting plane passing by the center of the heated spot. (c) Kinetics of the temperature rise in the area of maximal temperature elevation. Dotted line: experimental result. Solid line: optimized thermal model with $\delta = 0.48$ mm and $I = 77.8$ mW/cm^2.

TABLE I
THERMO-PHYSICAL PARAMETERS AND PENETRATION DEPTHS AT 60.4 GHZ IN AGAR AND PEP PHANTOMS, AND IN FOREARM SKIN

	k, W/(m·K)	ρ, kg/m^3	C, J/(kg·K)	δ_1, mm	δ_2, mm
Agar, 1%	0.565 [20]	1000	4180	0.32 ±0.03	0.32 ±0.01
Agar, 4%	0.548 [20]	1000	4012 *	0.34 ±0.04	0.34 ±0.01
PEP, 20%	0.52 [11]**	880	3636 [11]**	0.48 ±0.05	0.50 ±0.02
PEP, 25%	0.5 [11]	849	3500 [11]	0.60 ±0.01	0.61 ±0.03
Skin	0.335 [14]	1090 [19]	3507 [19]	0.49 ±0.03	0.49 ±0.03

δ_1 and δ_2 are the penetration depths of MMW determined from the temperature kinetics and direct permittivity measurements, respectively. ρ and C for the 1% agar case were accepted to be equal to those of water at the same temperature. *Linear extrapolation from data for water. **Linear extrapolation from data for 25% PEP phantom.

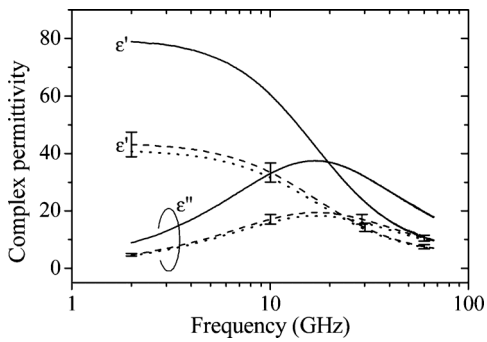

Fig. 4. Permittivity of water (solid lines) and 20% PEP (dotted lines) measured with a slim coaxial probe at 20 °C. Dashed lines: permittivity of 20% PEP phantom determined from heating kinetics measurements.

exposure. First, we determined the skin permittivity and the power reflection coefficient R. Then, we calculated I_0 as follows: $I_0 = I/(1-R)$. We found that, under the exposure conditions used in our study, $I_0 = 77$ mW/cm^2. As it was demonstrated previously that homogeneous models can be used to represent the skin at MMW [8], we use here the solution of BHTE obtained for a homogeneous and isotropic medium to fit the temperature kinetics. Since the distance from the waveguide aperture remains the same for all samples, I_0 is valid for all samples considered in this study.

We used literature data for k and C (Table I). In practice these values may not be as accurate as for other well-known materials. A parametric study has shown that the changes in δ and I are within $\pm 7\%$ when k and C are varied by $\pm 20\%$ (in reality, the uncertainty is expected to be much smaller). Thus, the exact knowledge of k and C is not critical for the accurate determination of δ and I. Moreover, the values of ρ were measured accurately for all phantoms. For the skin, we found that changes of blood flow produce a weak effect on the accuracy of δ and I (less than 0.4% when f_b is multiplied by a factor of four) if we use short records of the heating kinetics ($t \leq 10$ s).

IV. DISCUSSION

It is necessary to determine accurately the dielectric properties of skin and phantoms for near-future body-centric applications studies (e.g., antenna design in close proximity to the human body, on-body propagation channel characterization). Any uncertainty of these parameters could lead to errors in the power reflection and absorption at the air/skin or air/phantom interface, resulting therefore in an inaccurate evaluation of the interaction between on-body antennas and the human body. This could directly impact the performances of a wireless system.

In this study, we have demonstrated that the temperature kinetics measured using an IR camera can be used to determine the penetration depth and permittivity of high water content materials in the MMW range. The proposed procedure consists in fitting the solution of the BHTE to the measured temperature kinetics; this enables us to define I and δ. Then, for a given kinetics, a unique combination (I, δ) is found by minimizing the standard deviation.

The obtained values of δ are further used to calculate the skin and phantom permittivity spectra. It is worthwhile to note that the method used for the permittivity determination can be applied only to high-water-content materials with the same relaxation time as water. The dielectric properties of skin obtained with the new approach are in good agreement with the literature data [4], [8] and with permittivity spectra obtained from reflection measurements.

In this study, for the temperature measurements, we used a high-resolution IR camera. However, accurate temperature measurements could be also performed using either a thin thermocouple ($<$0.1 mm) or a fiber-optic temperature sensor. For a thermocouple, to perform an artifact-free temperature measurement, it is necessary to locate its leads perpendicular to the E-field of the incident electromagnetic wave [14]. Thermocouple-based measurements have an advantage over the IR thermometry because they measure temperature directly, and therefore they do not require to know the emissivity of the sample under test.

To validate the proposed methodology, we used two phantoms with dielectric properties close to those of skin, namely 20% and 25% PEP phantoms [3]. We found that the dielectric properties of the 20% PEP phantom are the closest ones to those of skin. Hence, this phantom can be used for modeling the interactions between the MMW and skin.

Finally, it is important to underline that this measurement technique can be easily and inexpensively implemented. In addition, compared with other in-house techniques based on reflection measurements [6]–[8], this approach uses low-cost commercially available equipment. It provides accurate results for the penetration depth and dielectric properties in a simple and fast way. Furthermore, the specific absorption rate in the near-surface layers can be directly determined using this approach.

REFERENCES

[1] R. C. Daniels, J. N. Murdock, T. S. Rappaport, and R. W. Heath, "60 GHz wireless: Up close and personal," *IEEE Microw. Mag.*, vol. 11, no. 7, pp. 44–50, Dec. 2010.
[2] S. L. Cotton, W. G. Scanlon, and P. S. Hall, "A simulated study of co-channel inter-BAN interference at 2.45 GHz and 60 GHz," in *Proc. Eur. Wireless Technol. Conf.*, Paris, France, Sep. 2010, pp. 61–64.
[3] N. Chahat, M. Zhadobov, S. Alekseev, and R. Sauleau, "Human skin-equivalent phantom for on-body antenna measurements in the 60 GHz band," *Electron. Lett.*, accepted for publication.
[4] S. Gabriel, R. W. Lau, and C. Gabriel, "The dielectric properties of biological tissues: III. Parametric models for the dielectric spectrum of tissues," *Phys. Med. Biol.*, vol. 41, pp. 2271–2293, 1996.

[5] O. P. Gandhi and A. Riazi, "Absorption of millimeter waves by human beings and its biological implications," *IEEE Trans. Microwave. Theory Tech.*, vol. MTT-34, no. 2, pp. 228–235, Feb. 1986.
[6] C. M. Alabaster, "Permittivity of human skin in millimetre wave band," *Electron. Lett.*, vol. 39, no. 21, pp. 1521–1522, Oct. 2003.
[7] H. Hwang, J. Yim, J.-W. Cho, C. Cheon, and Y. Kwon, "110 GHz broadband measurement of permittivity on human epidermis using 1 mm coaxial probe," in *IEEE Int. MTT-S Micro. Symp. Dig.*, Jun. 2003, vol. 1, pp. 399–402.
[8] S. I. Alekseev and M. C. Ziskin, "Human skin permittivity determined by millimeter wave reflection measurements," *Bioelectromagnetics*, vol. 28, no. 5, pp. 331–339, Jul. 2007.
[9] M. Zhadobov, N. Chahat, R. Sauleau, C. L. Quément, and Y. L. Dréan, "Millimeter-wave interactions with the human body: State of knowledge and recent advances," *Int. J. Microw. Wireless Technol.*, vol. 3, no. 2, pp. 237–247, Mar. 2011.
[10] W. J. Ellison, "Permittivity of pure water, at standard atmospheric pressure, over the frequency range 0–25 THZ and the temperature range 0–100°C," *J. Phys. Chem. Ref. Data*, vol. 36, no. 1, pp. 1–18, Feb. 2007.
[11] K. Ito, K. Furuya, Y. Okano, and L. Hamada, "Development and characteristics of a biological tissue-equivalent phantom for microwaves," *Electron. Commun. Japan*, vol. 84, no. 4, pp. 67–77, Apr. 2001.
[12] N. Chahat, M. Zhadobov, R. Sauleau, and K. Ito, "A compact UWB antenna for on-body applications," *IEEE Trans. Antennas Propag.*, vol. 59, no. 4, pp. 1123–1131, Apr. 2011.
[13] M. Zhadobov, R. Augustine, R. Sauleau, S. Alekseev, A. D. Paola, C. L. Quément, Y. S. Mahamoud, and Y. L. Dréan, "Complex permittivity of representative biological solutions in the 2–67 GHz range," *Bioelectromagnetics*, 2011, to be published.
[14] S. I. Alekseev and M. C. Ziskin, "Local heating of human skin by millimeter waves: A kinetics study," *Bioelectromagnetics*, vol. 24, no. 8, pp. 571–581, Oct. 2003.
[15] K. R. Foster, H. N. Kritikos, and H. P. Schwan, "Effect of surface cooling and blood flow on the microwave heating of tissue," *IEEE Trans. Biomed. Eng.*, vol. BME-25, no. 3, pp. 313–316, May 1978.
[16] E. H. Wissler, "Steady-state temperature distribution in man," *J. Appl. Physiol.*, vol. 16, no. 4, pp. 734–740, Jul. 1961.
[17] S. I. Alekseev, A. A. Radzievsky, M. K. Logani, and M. C. Ziskin, "Millimeter wave dosimetry of human skin," *Bioelectromagnetics*, vol. 29, no. 1, pp. 65–70, Jan. 2008.
[18] S. I. Alekseev, O. V. Gordiienko, and M. C. Ziskin, "Reflection and penetration depth in millimeter waves in murine skin," *Bioelectromagnetics*, vol. 29, no. 5, pp. 340–344, Jul. 2008.
[19] F. A. Duck, *Physical Properties of Tissue. A Comprehensive Reference Book*. San Diego, CA: Academic, 1990.
[20] M. Zhang, Z. Che, J. Chen, H. Zhao, L. Yang, Z. Zhong, and J. Lu, "Experimental determination of thermal conductivity of water-agar gel at different concentrations and temperatures," *J. Chem. Eng. Data*, vol. 56, no. 4, pp. 859–864, Apr. 2011.

Nacer Chahat (S'09) was born in Angers, France, in 1986. He received the degree in electrical engineering and radio communications and M.S. degree in telecommunication and electronics from the Ecole Supérieur d'ingénieurs de Rennes (ESIR), Rennes, France, in 2009. He is currently working toward the Ph.D. degree in signal processing and telecommunications at the Institute of Electronics and Telecommunications of Rennes (IETR), University of Rennes 1, Rennes, France.

He accomplished a six-month master's training period as a Special Research Student in 2009 at the Graduate School of Engineering, Chiba University, Chiba, Japan. His current research fields are electrically small antennas, millimeter-wave antennas, and the evaluation of the interaction between the electromagnetic field and human body.

Mr. Chahat was the recipient of the 2011 Best Poster Presentation Award from Bioelectromegnetics Society.

Maxim Zhadobov (S'05–M'07) received the M.S. degree in radiophysics from Nizhni Novgorod State University, Nizhni Novgorod, Russia, in 2003, and the Ph.D. degree in bioelectromagnetics from the Institute of Electronics and Telecommunications of Rennes (IETR), University of Rennes 1, Rennes, France, in 2006.

He performed post-doctoral training at the Center for Biomedical Physics, Temple University, Philadelphia, PA, in 2008 and then rejoined IETR as an Associate Researcher. He has authored or coauthored more than 70 scientific contributions. His main scientific interests are in the field of biocompatibility of electromagnetic radiations, including interactions of microwaves, millimeter waves, and pulsed radiations at the cellular level, health risks and environmental safety of emerging wireless communication systems, biocompatibility of wireless noninvasive biomedical techniques, therapeutic applications of nonionizing radiations, bioelectromagnetic optimization of body-centric wireless systems, and experimental and numerical electromagnetic dosimetry.

Dr. Zhadobov was the recipient of the 2005 Best Poster Presentation Award from the International School of Bioelectromagnetics, 2006 Best Scientific Paper Award from the Bioelectromegnetics Society, and Brittany's Young Scientist Award 2010.

Ronan Sauleau (M'04–SM'06) received the degree in electrical engineering and radio communications from the Institut National des Sciences Appliquées, Rennes, France, in 1995, the Agrégation degree from the Ecole Normale Supérieure de Cachan, France, in 1996, and the Ph.D. degree in signal processing and telecommunications and "Habilitation à Diriger des Recherche" degree from the University of Rennes 1, France, in 1999 and 2005, respectively.

He was an Assistant Professor and Associate Professor with the University of Rennes 1, Rennes, France, between September 2000 and November 2005 and again between December 2005 and October 2009. He has been a full Professor with the same university since November 2009. He holds five patents and is the author or coauthor of more than 100 journal papers and more than 240 publications in international conferences. His current research fields are numerical modelling (mainly FDTD), millimeter-wave printed and reconfigurable (MEMS) antennas, lens-based focusing devices, periodic and nonperiodic structures (electromagnetic bandgap materials, metamaterials, reflectarrays, and transmitarrays) and biological effects of millimeter waves.

Prof. Sauleau is a Junior member of the "Institut Universitaire de France." He received the 2004 ISAP Conference Young Researcher Scientist Fellowship (Japan) and the first Young Researcher Prize in Brittany, France, in 2001 for his research work on gain-enhanced Fabry–Perot antennas. He was awarded the Bronze medal by CNRS in 2008.

Stanislav I. Alekseev (M'10) received the M.S. degree in physics from Kazan State University, Kazan, Russia, in 1971, and the Ph.D. degree in biophysics from the Institute of Biophysics, Russian Academy of Sciences, Pushchino, Russia, in 1977.

He is currently a Senior Researcher with the Institute of Cell Biophysics, Russian Academy of Sciences, Pushchino, Russia, where he is involved in the research of neural effects of millimeter (mm)-wave irradiation. His research interests include theoretical and experimental study of microwave and mm-wave interaction with the skin, dosimetry and thermodynamics, mechanisms of microwave and mm-wave effects on model and neuronal membranes, on electrical activity of neurons, and cutaneous sensory afferents.